Brief Report

Optical coherence tomography based microangiography findings in hydroxychloroquine toxicity

Jason Kam[1], Qinqin Zhang[2], Jason Lin[1], Jin Liu[2], Ruikang K. Wang[1,2], Kasra Rezaei[1]

[1]Department of Ophthalmology, [2]Department of Bioengineering, University of Washington, Seattle, WA, USA

Correspondence to: Ruikang K. Wang, PhD. Department of Bioengineering, Department of Ophthalmology, University of Washington, Seattle, WA 98195, USA. Email: wangrk@uw.edu.

Abstract: Optical coherence tomography based microangiography (OMAG) is a new, non-invasive imaging modality capable of providing three dimentional (3D) retinal and choroidal microvascular maps without a need for exogenous dye. In this study, we evaluated the retinal and choroidal microvascular architecture of the macula in a patient with hydroxychloroquine (HCQ) toxicity using OMAG. Detailed microvascular information of the retina and the underlying choroid showed loss of parafoveal outer retinal vasculature with sparing of the central fovea vasculature.

Keywords: Optical coherence tomography-based angiography (OCT-based angiography); hydroxychloroquine toxicity; retinal vasculature

Introduction

Hydroxychloroquine (HCQ) is toxic to the retina in proportion to daily dose and duration of use, causing a characteristic Bull's eye retinopathy with loss of photoreceptors and retinal pigment epithelium (RPE) changes in the macula (1-3).

In 2011, the American Association of Ophthalmology (AAO) recommended new screening guidelines, which included multifocal electroretinography (mfERG), spectral domain optical coherence tomography (SD-OCT), fundus autofluorescence (FAF) and Swedish Interactive Threshold Algorithm (SITA) 10–2 automated field. Although the mechanism of this HCQ toxicity is unclear, as animal experiments have shown the drug can affect all retinal layers (4), the damage observed in clinical imaging is primarily to the outer retina (5).

With the novel and more sensitive imaging technology associated with SD-OCT, we utilized OCT-based microangiography (OMAG) as a non-invasive imaging modality to visualize the retinal and choroidal microvasculature (6-8). OMAG is sensitive to the movement of blood cells within the patent vessels to a level of capillary vessels, and thus providing three dimentional (3D) retinal microvascular networks that supply retinal and choroidal tissue *in vivo* (9,10). In this study, we investigated the retinal and choroidal microvasculature in a patient with HCQ toxicity.

Methods

The patient had a history of taking 400 mg of HCQ per day for 13 years without a dosage change. On the day of presentation she underwent a complete eye examination including slit lamp examination, fundus examination, Humphrey Visual Field 10–2, color funding imaging, digital FAF, and SD-OCT (Heidelberg Engineering GmbH, Heidelberg, Germany). The patient also underwent imaging with modified CIRRUS-5000 HD-OCT angiography prototype (Carl Zeiss Meditec Inc., Dublin, CA, USA) to acquire functional retinal vessel networks using the OMAG scanning protocol.

The OCT angiography system operated at a central wavelength of 840 nm and with an A-scan speed of

67,000 scans per second. Three scanning protocols were performed, which included a 512×128 macular raster scan for conventional 3D OCT image, a single high density B-scan with 1,024 A-scans to provide high definition OCT cross sectional image, and a montaging OMAG scan to acquire 6.5 mm × 6.5 mm 2 field of view microvascular image. The montage scan was achieved by using a motion tracking line scanning ophthalmoscope (LSO) built-in system and was composed of 3×3 single cube scans. Each cube had a field of view of 2.4 mm × 2.4 mm at the surface of retina. Transverse scanning was obtained with a total of 245 A-lines to form a single B scan. Four repeated B-scans were performed at each fixed location. Over a distance of 2.4 mm, 245 B scans were sampled with each scan measuring 9.8 microns apart. The acquisition rates were ~222 frames per second (fps). The OMAG algorithm (8,11) was applied to the volumetric dataset to obtain microstructural and microvascular images within the retina and choroid. The average OCT B-scans were examined in the regular OCT data to show cross-sections as well as en-face projections of the retinal tissue.

The retina and choroid were accurately segmented into different distinct physiologic layers using a semi-automatic segmentation software (12). Two layers were segmented in the retina: an inner layer from ganglion cell layer (GCL) to inner plexiform layer (IPL) which excluded the retinal nerve fiber layer (RNFL); and a deep layer from outer plexiform layer (OPL) to external limiting membrane (ELM). The choroidal segment contained both the choriocapillaris and choroidal layers. The segmentation was performed using the OCT cross sectional structural images based on the intensity differences of the retinal layers. The three dimensional structure of the retina and microvasculature were rendered and projected using a 3D visualization program coded with Matlab®.

Results

The 66-year-old Caucasian female with history of rheumatoid arthritis taking 400 mg/day of HCQ for 13 years with no prior eye examination or HCQ screening was referred for decreased vision in both eyes. Her best corrected visual acuity (BCVA) was 20/30 in both eyes. On examination, her weight was 55 kg and height was 157 cm. She denied any significant weight changes in the last 13 years (>10 lbs). Her most recent comprehensive metabolic panel (CMP) illustrated mild to moderate loss of kidney function with a glomerular filtration rate (GFR) of 50. Her liver

function was normal. She denied dosing changes of HCQ from the initiation of the drug.

The SD-OCT and FAF images showed the loss of parafoveal RPE with classic bull's-eye pattern in the right and left eye, respectively (*Figure 1*). Humphrey visual field test (HVF 10–2) demonstrated marked general depression in both eyes (*Figure 2*).

The OMAG enface images (*Figures 3,4*) demonstrated the loss of parafoveal deep microvasculature and choriocapillaris, the features of which are well comparable with the findings by SD-OCT, auto-fluorescence and HVF. The normal vascular ring around the foveal avascular zone (FAZ) was present in both eyes; however the capillary vascular density was dramatically reduced radially in the parafoveal area. The choroidal layers displayed increased intensity of microvasculature due to a window defect. This can be attributed to the atrophy of the RPE and outer retina in the parafoveal area consistent with this disease process (13).

Discussion

In this study, we utilized the OMAG imaging modality to investigate the retinal and choroidal microvascular architecture in a patient with HCQ toxicity. The resulting retinal images correlated well with the results obtained from SD-OCT, HVF and FAF. The OMAG has provided detailed information of parafoveal microvasculature mapping in our patient with HCQ toxicity. The deep parafoveal microvasculature displayed areas of capillary drop out when compared with the normal subjects. The appearance of outer retina in standard SD-OCT images and the RPE changes seen with FAF were consistent with the microvascular loss as observed in the OMAG images. OMAG is able to provide detailed information about the microvasculature in different layers of the retina and choroid. This imaging technique is noninvasive and objectively provides detailed images with a short capture time and enables the analysis of its correlation with the central visual deficiencies seen on HVF 10–2. OMAG may be useful as a novel screening method and early diagnostic tool for HCQ toxicity.

Conclusions

OMAG's ability to visualize microvasculature within retinal layers in HCQ may help facilitate the early assessment and diagnosis of disease and possibly provide better understanding of disease progression and efficacy for
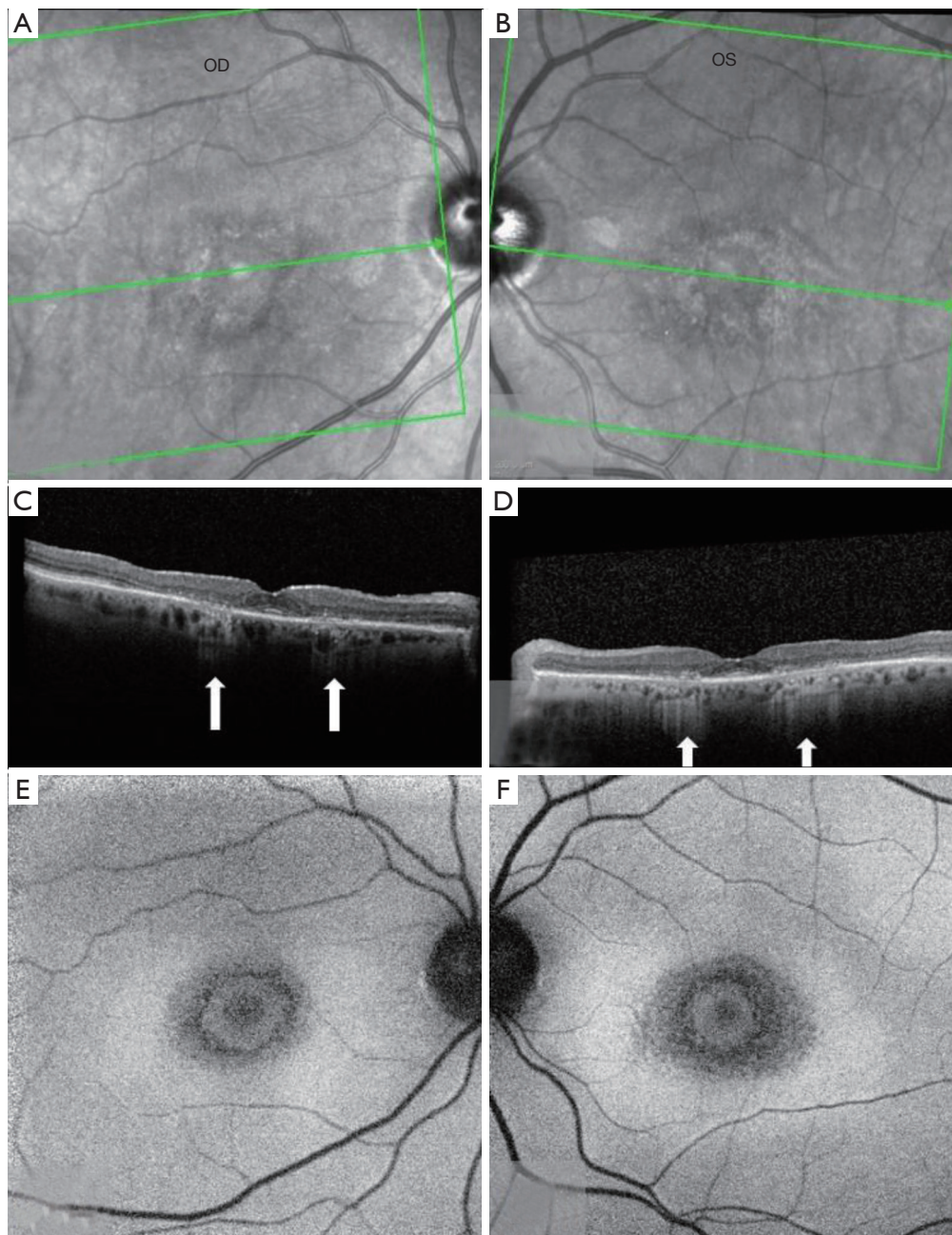
Figure 1 LSO (A,B) and SD-OCT cross-sectional images (C,D) demonstrate parafoveal thinning of the photoreceptor layers and loss of RPE and loss of ellipsoid segments in the same region with associated enhanced transmission defect into the choroid (arrows). The fundus autofluorescence images (E,F) show parafoveal hypo-autofluorescence due to loss of parafoveal RPE with classic bull's-eye pattern in the right and left eyes, respectively. LSO, line scanning ophthalmoscope; SD-OCT, spectral domain optical coherence tomography; RPE, retinal pigment epithelium.
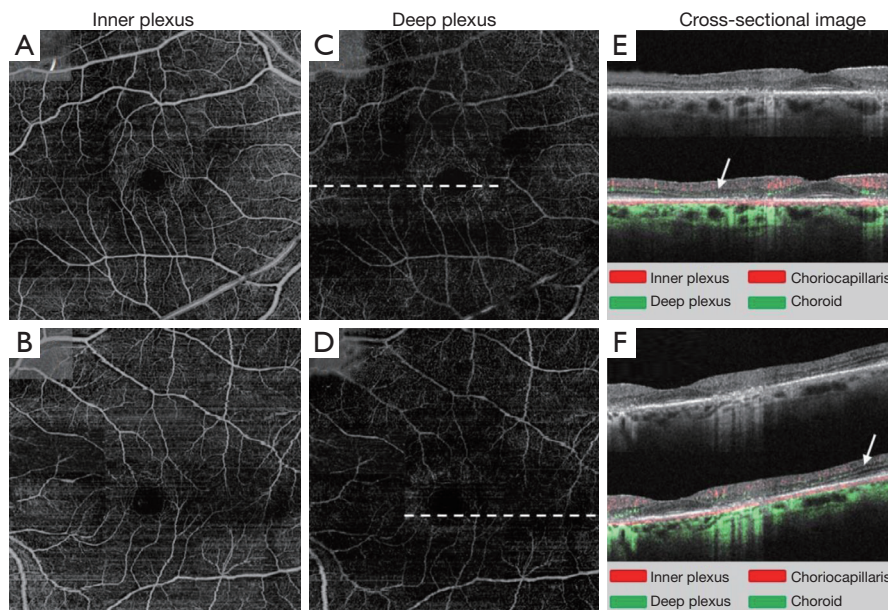
Figure 2 The automated SITA 10−2 visual field with marked general depression in right and left eyes, respectively. SITA, Swedish Interactive Threshold Algorithm.

Figure 3 OMAG retinal angiograms of the macular region of approximately 6.5 mm × 6.5 mm field of view: right eye (top row) and left eye (bottom row). Shown are the enface OMAGs for the inner (A,B) and deep plexus (C,D) within retina. (E,F) OCT-B scan structural image (top) together with overlaid flow signals (bottom) at the positions marks by dashed line in (B,E) are provided to appreciate the deterioration of retinal vasculature due to HCQ toxicity. The results show relatively normal vascular ring around the FAZ, however the capillary vascular density is almost absent in the parafovea and the outer retinal layers (arrows). OMAG, optical coherence tomography based microangiography; HCQ, hydroxychloroquine.
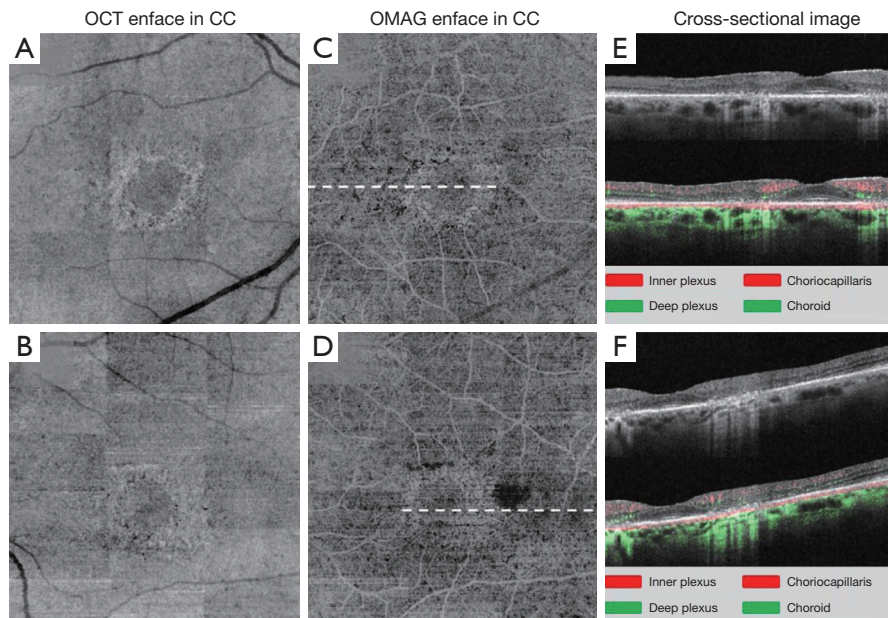

Figure 4 OMAG choroidal angiograms of the same macular region as in *Figure 3*: right eye (top row) and left eye (bottom row). OCT enface images (A,B) obtained from the CC slab (8 micron-slab beneath Bruch's membrane) demonstrate a ring shaped hyper-reflection OCT signals centered at the fovea. The corresponding OMAG images (C,D) of the choriocapillaris show loss of capillary vessels in the CC. (E,F) OCT-B scan structural image (top) together with overlaid flow signals (bottom) at the positions marks by dashed line in (C,D) are provided to appreciate the deterioration of choroidal vasculature due to HCQ toxicity. The OMAG displayed increased intensity of microvasculature of the choroidal layers from the choroidal vasculature exposure due to a window defect. OMAG, optical coherence tomography based microangiography; OCT, optical coherence tomography; HCQ, hydroxychloroquine.

potential future treatment. OMAG is a newer form of non-invasive imaging technology that promises the investigation of certain retinal and optical nerve pathologies. It is as safe as current SD-OCT and does not require exogenous dye injection. This study illustrates the ability of OMAG to evaluate the retinal and choroidal microvasculature consistent with findings of current standards.

Footnote

Conflicts of Interest: The authors have no conflicts of interest to declare.

References

1. Melles RB, Marmor MF. The risk of toxic retinopathy in patients on long-term hydroxychloroquine therapy. JAMA Ophthalmol 2014;132:1453-60.
2. Melles RB, Marmor MF. Pericentral retinopathy and racial differences in hydroxychloroquine toxicity. Ophthalmology 2015;122:110-6.
3. Mavrikakis I, Sfikakis PP, Mavrikakis E, Rougas K, Nikolaou A, Kostopoulos C. The Incidence of irreversible retinal toxicity in patients treated with hydroxychloroquine: a reappraisal. Ophthalmology 2003;110:1321-6.
4. Marmor MF. Comparison of screening procedures in hydroxy-chloroquine toxicity. Arch Ophthalmol 2012;130:461-9.
5. Rosenthal AR, Kolb H, Bergsma D, Huxsoll D, Hopkins JL. Chloroquine retinopathy in the rhesus monkey. Invest Ophthalmol Vis Sci 1978;17:1158-75.
6. Wang RK, Jacques SL, Ma Z, Hurst S, Hanson SR, Gruber A. Three dimensional optical angiography. Opt Express 2007;15:4083-97.
7. An L, Shen TT, Wang RK. Using ultrahigh sensitive optical microangiography to achieve comprehensive depth resolved microvasculature mapping for human retina. J Biomed Opt 2011;16:106013.
8. Zhang A, Zhang Q, Chen CL, Wang RK. Methods and algorithms for optical coherence tomography-based angiography: a review and comparison. J Biomed Opt 2015;20:100901.
9. Wang RK. Optical Microangiography: A Label Free 3D Imaging Technology to Visualize and Quantify Blood Circulations within Tissue Beds in vivo. IEEE J Sel Top Quantum Electron 2010;16:545-54.
10. Reif R, Wang RK. Label-free imaging of blood vessel morphology with capillary resolution using optical microangiography. Quant Imaging Med Surg 2012;2:207-12.
11. Huang Y, Zhang Q, Thorell MR, An L, Durbin MK, Laron M. Swept-source OCT angiography of the retinal vasculature using intensity differentiation-based optical microangiography algorithms. Ophthalmic Surg Lasers Imaging Retina 2014;45:382-9.
12. Yin X, Chao JR, Wang RK. User-guided segmentation for volumetric retinal optical coherence tomography images. J Biomed Opt 2014;19:086020.
13. de Sisternes L, Hu J, Rubin DL, Marmor MF. Localization of damage in progressive hydroxychloroquine retinopathy on and off the drug: inner versus outer retina, parafovea versus peripheral fovea. Invest Ophthalmol Vis Sci 2015;56:3415-26.